Filtering Crosstalk from Bath Non-Markovianity via Spacetime Classical Shadows

G. A. L. White,[1,2,*] K. Modi,[2,3,†] and C. D. Hill[1,4,5,‡]
[1]School of Physics, University of Melbourne, Parkville, Victoria 3010, Australia
[2]School of Physics and Astronomy, Monash University, Clayton, Victoria 3800, Australia
[3]Centre for Quantum Technology, Transport for New South Wales, Sydney, New South Wales 2000, Australia
[4]School of Mathematics and Statistics, University of Melbourne, Parkville, Victoria, 3010, Australia
[5]Silicon Quantum Computing, The University of New South Wales, Sydney, New South Wales 2052, Australia

(Received 25 November 2022; accepted 2 March 2023; published 20 April 2023)

From an open system perspective non-Markovian effects due to a nearby bath or neighboring qubits are dynamically equivalent. However, there is a conceptual distinction to account for: neighboring qubits may be controlled. We combine recent advances in non-Markovian quantum process tomography with the framework of classical shadows to characterize spatiotemporal quantum correlations. Observables here constitute operations applied to the system, where the free operation is the maximally depolarizing channel. Using this as a causal break, we systematically erase causal pathways to narrow down the progenitors of temporal correlations. We show that one application of this is to filter out the effects of crosstalk and probe only non-Markovianity from an inaccessible bath. It also provides a lens on spatiotemporally spreading correlated noise throughout a lattice from common environments. We demonstrate both examples on synthetic data. Owing to the scaling of classical shadows, we can erase arbitrarily many neighboring qubits at no extra cost. Our procedure is thus efficient and amenable to systems even with all-to-all interactions.

DOI: 10.1103/PhysRevLett.130.160401

Introduction.—In the race to fault tolerant quantum computing, magnified sensitivity to complex dynamics in open quantum systems requires increasingly tailored characterization and spectroscopic techniques [1–8]. Correlated dynamics are one particularly pernicious class of noise, and can be generated from a variety of sources, including inhomogeneous magnetic fields, coherent bath defects, and nearby qubits, see Fig. 1(a) [9,10]. Concerningly, these effects are often omitted from quantum error correction noise models despite being ubiquitous in noisy intermediate-scale quantum (NISQ) hardware [5,6,11–14].

Temporal—or non-Markovian—correlations are elements of error that are correlated between different points in time, as mediated by interactions with an external system [6,15]. A process is said to be non-Markovian if the total dynamics do not factorize into a product of dynamical maps [16], a stronger condition than the well-known completely positive divisibility of dynamics [17]. The specific mediator of these effects is both conceptually and experimentally relevant device information. Is it controllable, or is it part of the inaccessible bath? Relatedly, if the dynamics of two nearby qubits do not spatially factorize, this is known as crosstalk. If one qubit is traced out, then entangling crosstalk—such as the always-on ZZ interactions in transmon qubits [18]—can generate temporal correlations for the second qubit. Whether the dynamics look non-Markovian depends on whether it is feasible or not to dilate the characterization to multiple qubits and account for the variables responsible for these correlations.

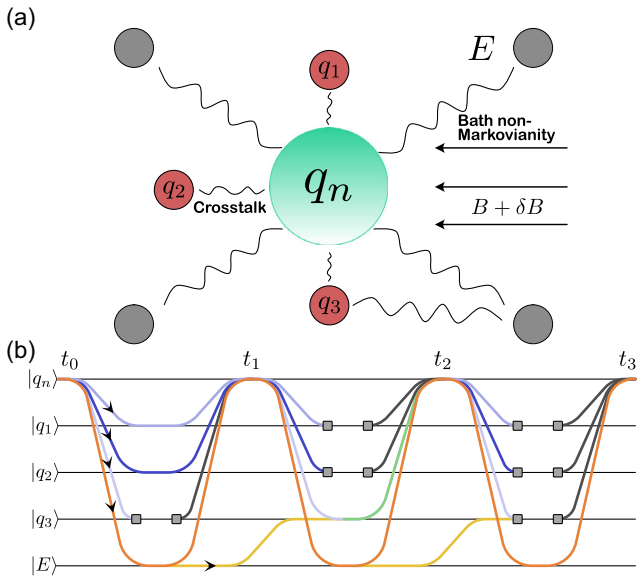

FIG. 1. System of interacting qubits and an inaccessible non-Markovian environment (E). (a) A target qubit q_n may interact via crosstalk mechanisms with other qubits, $\{q_1, q_2, q_3, \cdots\}$, in a quantum device, as well as defects in the bath and fluctuating classical fields $B + \delta B$. (b) The non-Markovian correlations for that system may be separated into different causal pathways by which the correlations are mediated. Causal breaks (depicted in gray) erase any temporal correlations from a given pathway, allowing one to infer the various contributions to total non-Markovianity from nearby qubits and environment.

Typically, it is not. Since crosstalk and bath non-Markovianity can easily be conflated, it is crucial to find robust methods that can not only account for their behavior, but distinguish them.

In this Letter, we establish a systematic, concrete, and efficient approach to the two pragmatic questions: (i) if non-Markovian dynamics are detected across different timescales for a qubit, do they come from neighboring qubits or a nearby bath? And (ii) how can we determine when two qubits are coupled to a shared bath generating common cause non-Markovian effects. The solutions here have highly practical implications. Namely, whether curbing the correlated effects is achievable through control or fabrication methods [19,20]. Process tensor tomography (PTT) is a recently developed generalization to quantum process tomography, and can guarantee an answer to these questions and more, but the number of experiments required grows as $\mathcal{O}(d^{2kn+N})$ to find correlations across k steps over N qudits [6].

The basic premise of our Letter is to apply the method of classical shadows [21] to PTT, resolving these problems. The classical shadow philosophy implements randomized single-shot measurements to learn properties of a state, granting access to an exponentially larger pool of observables at fixed locality. Employing this, instead of reconstructing the whole multitime process for an entire quantum register, we can estimate and analyze each of the fixed-weight process marginals. Marginalizing over a measurement is equivalent to measuring and throwing the outcome away. To marginalize over a process input is equivalent to inputting a maximally mixed state. Hence, these are maximal depolarizing channels at no extra cost, which act as causal breaks on controllable systems.

When suitably placed, these operations eliminate temporal correlations as mediated on the chosen Hilbert spaces, thus allowing non-Markovian sources to be causally tested. We illustrate this idea in Fig. 1(b). The end result is the simultaneous determination of the bath-mediated non-Markovianity on all qubits. Our approach hence only depends on the individual system size (in this Letter, qubits), and is a physics-independent way for us to test the relevant hypotheses. We are also able to simultaneously compute all spacetime marginals, extending the randomized measurement toolkit to the spatiotemporal domain [22].

Spatiotemporal classical shadows.—By virtue of the state-process equivalence for multitime processes [15,23–25], quantum operations on different parts of a system at different times constitute observables on a many-body quantum state. This allows state-of-the-art characterization techniques to be applied to quantum stochastic processes. Classical shadow tomography [21,22] is one such technique, and already has many generalizations and applications [26–29]. Measuring classical shadows allows for exponentially greater observables to be determined about a state, provided sufficiently low weight. But this restriction means the technique has limitations for the study of temporal correlations (which are high weight) in contrast to spatial ones, as discussed in Ref. [12]. Our Letter expands on this to the multiqubit–multitime case, and identifies other desirable applications of classical shadows to multitime processes.

Definitions and notation: Consider a quantum device with a register of qudits $\mathbf{Q} \coloneqq \{q_1, q_2, \ldots, q_N\}$ across a series of times $\mathbf{T}_k \coloneqq \{t_0, t_1, \ldots, t_k\}$. We take the whole quantum device to define the system: $\mathcal{H}_S \coloneqq \bigotimes_{j=1}^{N} \mathcal{H}_{q_j}$. The device interacts with an external, inaccessible environment whose space we denote $\mathcal{H}_E$. The k-step open process is driven by a sequence $\mathbf{A}_{k-1:0}$ of control operations on the whole register, each represented mathematically by completely positive (CP) maps: $\mathbf{A}_{k-1:0} \coloneqq \{\mathcal{A}_0, \mathcal{A}_1, \ldots, \mathcal{A}_{k-1}\}$, after which one obtains a final state $\rho_k^S(\mathbf{A}_{k-1:0})$ conditioned on this choice of interventions. Note that where we label an object with time information only, that object is assumed to concern the entire register. These controlled dynamics have the form

$$\rho_k^S(\mathbf{A}_{k-1:0}) = \mathrm{Tr}_E[U_{k:k-1}\mathcal{A}_{k-1}\cdots U_{1:0}\mathcal{A}_0(\rho_0^{SE})], \quad (1)$$

where $U_{k:k-1}(\cdot) = u_{k:k-1}(\cdot)u_{k:k-1}^{\dagger}$. Now let the Choi representations of each $\mathcal{A}_j$ be denoted by a caret, i.e., $\hat{\mathcal{A}}_j = \mathcal{A}_j \otimes \mathcal{I}[|\Phi^+\rangle\langle\Phi^+|] = \sum_{nm} \mathcal{A}_j[|n\rangle\langle m|] \otimes |n\rangle\langle m|$. Then, the driven process in Eq. (1) for arbitrary $\mathbf{A}_{k-1:0}$ uniquely defines a multilinear mapping across the register $\mathbf{Q}$—called a process tensor, $\Upsilon_{k:0}$—via a generalized Born rule [15,24]:

$$p_k^S(\mathbf{A}_{k-1:0}) = \mathrm{Tr}[\Upsilon_{k:0}(\Pi_k \otimes \hat{\mathcal{A}}_{k-1} \otimes \cdots \hat{\mathcal{A}}_0)^{\mathrm{T}}]. \quad (2)$$

At each time t_j, the process has an output index $\mathfrak{o}_j$ (which is measured), and input index $\mathfrak{i}_{j+1}$ (which feeds back into the process). The details of process tensors can be found in the Supplemental Material [30], but are not crucial to understanding this Letter. The two important properties that we stress are (i) a sequence of operations constitutes an observable on the process tensor via Eq. (2), generating the connection to classical shadows, and (ii) a process tensor forms a collection of possibly correlated completely positive, trace-preserving (CPTP) maps, and hence may be marginalized in both time and space to yield the jth CPTP map describing the dynamics of the ith qubit $\hat{\mathcal{E}}_{j:j-1}^{(q_i)}$. A process is said to be Markovian if and only if its process tensor is a product state across time. The measure of non-Markovianity we use throughout this Letter is that described in Ref. [16]. Specifically, it is the relative entropy $S[\rho\|\sigma] = \mathrm{Tr}[\rho(\log\rho - \log\sigma)]$ between a process tensor $\Upsilon_{k:0}$ and its closest Markov description, the product of its marginals:

$$\Upsilon_{k:0}^{(\mathrm{Markov})} = \hat{\mathcal{E}}_{k:k-1} \otimes \cdots \otimes \hat{\mathcal{E}}_{1:0} \otimes \rho_0. \quad (3)$$

We denote this generalized quantum mutual information (QMI) for a given process by $\mathcal{N}(\Upsilon_{k:0})$. Classical shadow tomography provides access to a small number of low weight observables, with $\langle\mathbb{I}\rangle$ on the remainder of the subsystems. The case where $\langle\mathbb{I}_{\mathbf{i}_{j+1}}\mathbb{I}_{\mathfrak{o}_j}\rangle$ is evaluated is equivalent to selecting an $\hat{A}_j = \mathbb{I}_{\mathbf{i}_{j+1}} \otimes \mathbb{I}_{\mathfrak{o}_j} \equiv \mathbb{I}_{\mathbf{i}_{j+1}\mathfrak{o}_j}$. This is the Choi state of the maximal depolarizing channel, up to normalization. When marginalizing across all but a handful of times or qubits, we will denote the remaining steps or registers by commas, i.e.,

$$\hat{\mathcal{E}}^{(q_{i_0},q_{i_1})}_{j_0:\ j_0-1,j_1:j_1-1} \coloneqq \mathrm{Tr}_{\{\overline{q_{i_0}},\overline{q_{i_1}}\},\{\overline{t_{j_0}},\overline{t_{j_0-1}},\overline{t_{j_1}},\overline{t_{j_1-1}}\}}[\Upsilon_{k:0}];$$
$$\Upsilon^{(q_i)}_{k:0} = \mathrm{Tr}_{\overline{q_i}}[\Upsilon_{k:0}], \tag{4}$$

where the overlines denote complement, i.e., every qubit except q_i: $\mathbf{Q}\backslash\{q_i\}$, or every time except t_j: $\mathbf{T}_k\backslash\{t_j\}$.

When non-Markovian correlations persist as mediated by the inaccessible bath, we designate this as bath non-Markovianity (BNM). When the correlations are mediated from neighboring qubits, we designate this as register non-Markovianity (RNM). Naturally, since the bath cannot be controlled by definition, BNM can be probed without RNM, but RNM effects cannot be isolated by themselves. Instead, one might consider the spatial process marginals alone to measure direct crosstalk [26,32,33].

Procedure: To map these correlations on each qubit, the classical shadows procedure naturally extends as follows: at each $t \in \mathbf{T}_k$, on each $q \in \mathbf{Q}$, apply a unitary operation randomly selected from the single qubit Clifford group, followed by a projective measurement in the Z basis. This defines a POVM on all qubits across all times $\{U_i^\dagger|x\rangle\langle x|U_i\}^{q_m}_{t_j}$. The measurements considered have four defining features: the qubit q on which they act, the time t at which they are implemented, and the basis change U applied prior to a measurement outcome x. To avoid notational overload, we omit these final two labels when writing instruments where the context is clear.

Record both the outcome of the measurement and the random unitary. Reset the qubit to state $|0\rangle$ and apply a random Clifford gate, recording this operation as well. The intended effect of this is to apply a randomized quantum instrument—i.e., a random measurement with an independently random postmeasurement state. See Fig. 2 for the circuit diagram. The application of an instrument in each chosen location in space and time constitutes a single-shot piece of information about the process tensor. The single shot is a projection of the process tensor onto the sequence of interleaving measurements Π and preparations P:

$$\hat{\mathbf{\Pi}}_{\mathbf{T}_k} = \bigotimes_{l=0}^{k}\bigotimes_{j=1}^{N}(U^{j*}_{\mathfrak{o}_l}|x\rangle\langle x|U^{j\mathrm{T}}_{\mathfrak{o}_l}),$$
$$\hat{\mathbf{P}}_{\mathbf{T}_k} = \bigotimes_{l=1}^{k}\bigotimes_{j=1}^{N}(U^{j}_{\mathbf{i}_l}|0\rangle\langle 0|U^{j\dagger}_{\mathbf{i}_l}), \tag{5}$$

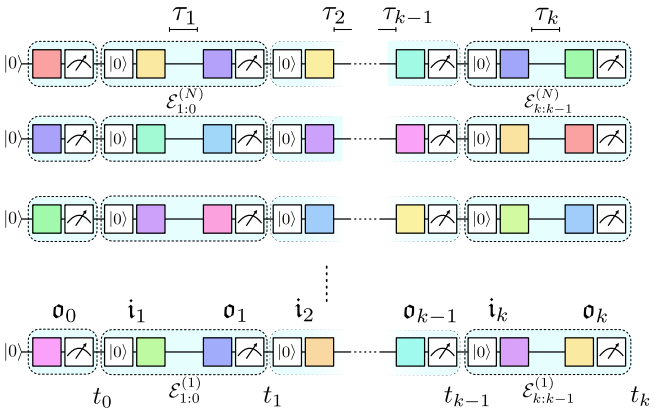

FIG. 2. Circuit diagram of our proposed procedure. Spatiotemporal classical shadows can be obtained by applying random Clifford operations to each qubit, projectively measuring, resetting, and then a random Clifford preparation. By repeating these instruments across the circuit with chosen wait times, the appropriate shadow postprocessing may be used to determine spatiotemporal marginals of the process. Each $\mathfrak{o}_j$ signifies an index where the state of the system is read out at time t_j, and each $\mathbf{i}_{j+1}$ signifies the preparation of a new state, also at time t_j.

with probability given in accordance with Eq. (2). Note that the Choi state of a POVM element is given by its transpose [34]: $\hat{\Pi} = \Pi^{\mathrm{T}}$. Using the tensor product structure, we can examine each measurement and each preparation at each time on each qubit separately. The preparations $P^{q_j}_l$ are all deterministic, and enact the quantum channel

$$\mathcal{M}_{\mathcal{P}}(\sigma^{q_j}_{\mathbf{i}_l}) = \mathbb{E}_{U^j_{\mathbf{i}_l}\sim\mathcal{U}}[U^j_{\mathbf{i}_l}|0\rangle\langle 0|U^{j\dagger}_{\mathbf{i}_l}], \tag{6}$$

where $\mathbb{E}_{U^j_{\mathbf{i}_l}\sim\mathcal{U}}$ is the expectation value taken over the unitary ensemble. The inverse of this gives the classical shadow on the process input legs

$$\hat{D}^j_{\mathbf{i}_l} \coloneqq \mathcal{M}^{-1}_{\mathcal{P}}(U^j_{\mathbf{i}_l}|0\rangle\langle 0|U^{j\dagger}_{\mathbf{i}_l}) = 3U^j_{\mathbf{i}_l}|0\rangle\langle 0|U^{j\dagger}_{\mathbf{i}_l} - \mathbb{I}. \tag{7}$$

Existence of this inverse is guaranteed by tomographic completeness of the ensemble [21]. For the measurements $\Pi^{q_j}_l$ we have the usual single qubit Clifford channel:

$$\mathcal{M}_{\mathcal{D}}(\sigma^{q_j}_{\mathfrak{o}_l}) = \mathbb{E}_{U^j_{\mathfrak{o}_l}\sim\mathcal{U},x\sim\mathrm{Tr}[\Pi^{q_j}_l\sigma^{q_j}_{\mathfrak{o}_l}]}[U^{j*}_{\mathfrak{o}_l}|x\rangle\langle x|U^{j\mathrm{T}}_{\mathfrak{o}_l}]. \tag{8}$$

Here, $|x\rangle$ on each qubit at each time is sampled according to the generalized Born rule in Eq. (2), and depends generally on the operations that come before it. The inverse of this channel gives the shadow on the output legs:

$$\hat{\Delta}^j_{\mathfrak{o}_l} \coloneqq \mathcal{M}^{-1}_{\mathcal{D}}(U^{j*}_{\mathfrak{o}_l}|x\rangle\langle x|U^{j\mathrm{T}}_{\mathfrak{o}_l}) = 3U^{j*}_{\mathfrak{o}_l}|x\rangle\langle x|U^{j\mathrm{T}}_{\mathfrak{o}_l} - \mathbb{I}. \tag{9}$$

Hence, for a k-step process on N qubits, the classical shadow is a reshuffling of

$$\hat{\Upsilon}_{k:0} = \hat{\mathbf{D}}^{\mathrm{T}}_{\mathbf{T}_k} \otimes \hat{\mathbf{\Delta}}^{\mathrm{T}}_{\mathbf{T}_k}, \tag{10}$$

to have the $\mathfrak{o}$ and $\mathfrak{i}$ legs alternating, and from which properties can be efficiently determined using the usual median-of-means estimation described in Ref. [21].

Erasing non-Markovian pathways.—The above procedure suffices to estimate marginals of a process tensor with only logarithmic overhead, which we show for completeness in the Supplemental Material [30]. In short, we estimate the required observables to uniquely fix the process marginal, and then employ a maximum likelihood algorithm to determine a physically consistent process tensor. We consider two possible applications of spatiotemporal classical shadows, supplemented by numerical demonstrations.

Distinguishing between passive crosstalk and bath non-Markovianity: First, we consider certifying when non-Markovian correlations originate via an inaccessible bath, or from neighboring qubits in the register. Certifying bath non-Markovianity means estimating $\Upsilon^{(q_i)}_{k:0}$—the marginal process tensor for a single qubit. This can be simultaneously performed for all $q_i \in \mathbf{Q}$. The Choi state of the operations on the remainder of the qubits at each time will be $\mathbb{I}/d$, i.e., a maximally depolarizing channel. Because this enacts a causal break any information traveling from the system into the register cannot persist forward in time. Hence, computing $\mathcal{N}(\Upsilon^{(q_i)}_{k:0})$ will be a measure of correlations from an inaccessible bath alone. We formally show this in the Supplemental Material [30].

We demonstrate this numerically in Fig. 3. Here, we have 15 qubits and one defect quantum system acting as the bath in a two-step process, and then compute $\mathcal{N}(\Upsilon^{q_i}_{2:0})$. The qubits each experience a random nearest-neighbor ZZ-coupling crosstalk, and the ones geometrically closest to the defect are Heisenberg coupled to that system: $H = \sum_i \sum_\alpha J^\alpha_{i,E} \sigma^{(i)}_\alpha \sigma^{(E)}_\alpha$ for random $J^\alpha_{i,E}$. Figure 3(a) shows the standard fare: estimating the process tensor of each qubit and determining its non-Markovianity while the other qubits remain idle. However, the results are not so informative because they do not distinguish between RNM and BNM effects, and so every qubit experiences temporal correlations. Figure 3(b) shows the results of a shadow marginal estimation, and we readily identify only the qubits coupled to bath defects have a nonzero $\mathcal{N}(\Upsilon^{(q_i)}_{2:0})$.

Identifying shared baths: A second important scenario we consider is where two qubits are correlated via common cause from a shared bath. For example, this might be experiencing the same stray magnetic field inhomogeneities or through a coupling to a common defect. This is sometimes referred to as crosstalk, because the joint map $\hat{\mathcal{E}}^{(q_1,q_2)}_{j:j-1}$ does not factor to $\hat{\mathcal{E}}^{(q_1)}_{j:j-1} \otimes \hat{\mathcal{E}}^{(q_2)}_{j:j-1}$ [32]. However,

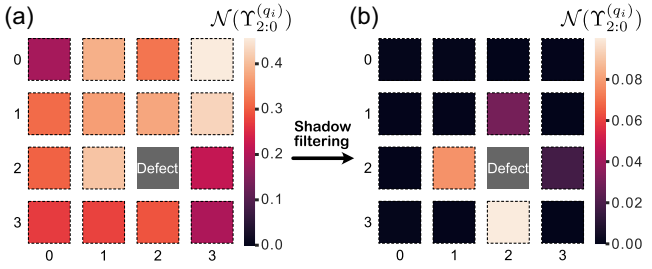

FIG. 3. A numerical simulation demonstrating the proposed technique to isolate environmental effects. A grid of 15 qubits is simulated with crosstalk effects and an inaccessible non-Markovian defect. (a) Determining the non-Markovianity on each qubit individually (with the remainder idle) is not very informative, since each qubit looks non-Markovian due to passive crosstalk. (b) After learning all of the shadow marginals $\Upsilon^{(q_j)}_{2:0}$, the crosstalk is filtered out to reveal which qubits possess temporal correlations from the environment.

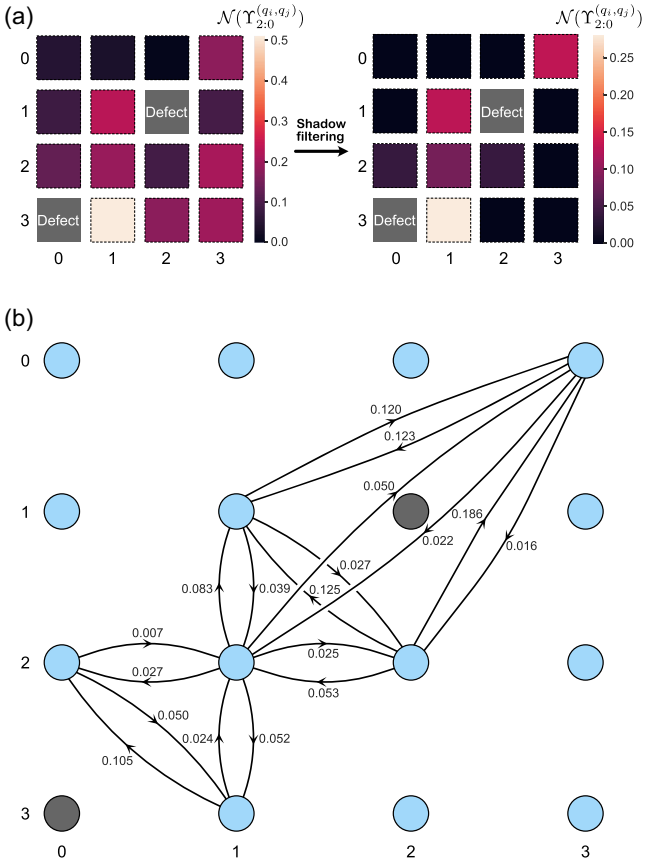

FIG. 4. A numerical simulation demonstrating the proposed technique to determine qubits with shared baths. A grid of 14 qubits is simulated with crosstalk effects and two inaccessible non-Markovian defects. (a) Shadow filtering may be used to find qubits coupled to an inaccessible bath as before. (b) By looking at the correlations between map $\hat{\mathcal{E}}^{(q_m)}_{1:0}$ with $\hat{\mathcal{E}}^{(q_n)}_{2:1}$, we can infer which qubits share common baths and the extent to which the defects redistribute quantum information. Note, the relationship lines between qubits are not direct crosstalk interactions, but bath-mediated spatiotemporal correlation.

we consider this a coarse description because neither system acts as a direct cause for each other's dynamics. Instead, they are subject to spatiotemporal correlations as mediated by the same non-Markovian bath. The key, therefore, is to measure the relationship between the maps $\hat{\mathcal{E}}^{(q_1)}_{j:j-1}$ and $\hat{\mathcal{E}}^{(q_2)}_{j+1:j}$.

We demonstrate this numerically in Fig. 4. We have a similar setup to before, except this time with two bath defects. Performing a shadow filtering [Fig. 4(a)] again reveals which qubits are coupled to the defects. However, in Fig. 4(b), we look at the spacetime marginals estimated from the shadow data. This fine-grained data indicate which qubits are commonly coupled to bath defects, versus independently coupled. The arrows from qubit q_i to qubit q_j indicate the QMI in the process with marginals $\hat{\mathcal{E}}^{(q_j)}_{2:1} \otimes \Upsilon^{(q_i)}_{1:0}$, where $\Upsilon_{1:0}$ also includes initial correlations. The erasure of q_j in the first step and q_i in the second step eliminates the possibility of direct-cause correlations between the two qubits, leaving only the possibility of common cause. In other words, nonzero values are a measure of non-Markovian correlations distributed by a shared bath between two qubits. This generates a more informative view of the connected interplay between qubits and their environment.

Discussion.—We have introduced a scalable and conceptually simple method to distinguish between non-Markovian dynamics generated by nearby qubits in a quantum device, and those from an inaccessible bath. This contributes to the growing zoo of quantum benchmarking techniques, and yet satisfies a unique niche. Geometrically isolating non-Markovian sources across a device can inform various facets of the development process: the signals can warrant further investigation and inform the fabrication process; flag qubits to be given extra control attention; and be fed forward to error-correction decoders.

This also extends the capabilities of the randomized measurement toolbox to the multitime and multiqubit domain, and we have identified an important use case in efficient casual testing. We anticipate that there exist many alternate applications of classical shadows to spatiotemporal quantum states beyond what we have discussed here. Notably, classical shadows have seen extensive recent generalization and application to quantum speed-up in the determination of quantum properties [22,28,35,36]. Dynamic sampling of small systems, meanwhile, has been shown to be complex in the multitime sampling setting [37]. We provide a template by which a similar approach may be applied to quantum stochastic processes. The learning of spatiotemporal correlations constitutes the most general platform for this task, combining many-body states with multitime processes.

Further research is needed to explore alternative ensembles suitable for multitime processes. Specifically, whether it is tractable to efficiently learn global observables; which properties provide useful information about the non-Markovian interactions; and whether causality conditions imply a learnability gap between quantum states and quantum processes.

We note also that we have introduced our filter in full generality with respect to PTT, but the techniques are generic: the only important point is that causal breaks are applied to neighboring qubits between each step. The same principles will broadly apply to other approaches to learning non-Markovian dynamics [3,38–40].

This work was supported by the University of Melbourne through the establishment of an IBM Quantum Network Hub at the University. G. A. L. W. is supported by an Australian Government Research Training Program Scholarship. C. D. H. is supported through a Laby Foundation grant at The University of Melbourne. K. M. is supported through Australian Research Council Discovery Project DP22010179. K. M. and C. D. H. acknowledge the support of the Australian Research Council's Discovery Project DP210100597. K. M. and C. D. H. were recipients of the International Quantum U Tech Accelerator award by the U.S. Air Force Research Laboratory. C. D. H's contributions to this project were carried out while he was affiliated with The University of Melbourne.

*greg.white@monash.edu
†kavan.modi@monash.edu
‡charles.hill1@unsw.edu.au

[1] T. Chalermpusitarak, B. Tonekaboni, Y. Wang, L. M. Norris, L. Viola, and G. A. Paz-Silva, PRX Quantum **2**, 030315 (2021).
[2] C. Ferrie, C. Granade, G. Paz-Silva, and H. M. Wiseman, New J. Phys. **20**, 123005 (2018).
[3] E. Nielsen, J. K. Gamble, K. Rudinger, T. Scholten, K. Young, and R. Blume-Kohout, Quantum **5**, 557 (2021).
[4] K. Rudinger, T. Proctor, D. Langharst, M. Sarovar, K. Young, and R. Blume-Kohout, Phys. Rev. X **9**, 021045 (2019).
[5] G. A. L. White, C. D. Hill, F. A. Pollock, L. C. L. Hollenberg, and K. Modi, Nat. Commun. **11**, 6301 (2020).
[6] G. A. L. White, F. A. Pollock, L. C. L. Hollenberg, K. Modi, and C. D. Hill, PRX Quantum **3**, 020344 (2022).
[7] A. Youssry, G. A. Paz-Silva, and C. Ferrie, npj Quantum Inf. **6**, 95 (2020).
[8] U. von Lüpke, F. Beaudoin, L. M. Norris, Y. Sung, R. Winik, J. Y. Qiu, M. Kjaergaard, D. Kim, J. Yoder, S. Gustavsson, L. Viola, and W. D. Oliver, PRX Quantum **1**, 010305 (2020).
[9] E. Paladino, Y. M. Galperin, G. Falci, and B. L. Altshuler, Rev. Mod. Phys. **86**, 361 (2014).
[10] S. Mavadia, C. Edmunds, C. Hempel, H. Ball, F. Roy, T. Stace, and M. Biercuk, npj Quantum Inf. **4**, 7 (2018).
[11] B. D. Clader, C. J. Trout, J. P. Barnes, K. Schultz, G. Quiroz, and P. Titum, Phys. Rev. A **103**, 052428 (2021).

[12] G. A. L. White, F. A. Pollock, L. C. L. Hollenberg, C. D. Hill, and K. Modi, arXiv:2107.13934.
[13] N. H. Nickerson and B. J. Brown, Quantum **3**, 131 (2019).
[14] R. Harper, S. T. Flammia, and J. J. Wallman, Nat. Phys. **16**, 1184 (2020).
[15] F. A. Pollock, C. Rodríguez-Rosario, T. Frauenheim, M. Paternostro, and K. Modi, Phys. Rev. A **97**, 012127 (2018).
[16] F. A. Pollock, C. Rodríguez-Rosario, T. Frauenheim, M. Paternostro, and K. Modi, Phys. Rev. Lett. **120**, 040405 (2018).
[17] S. Milz, M. S. Kim, F. A. Pollock, and K. Modi, Phys. Rev. Lett. **123**, 040401 (2019).
[18] E. Magesan and J. M. Gambetta, Phys. Rev. A **101**, 052308 (2020).
[19] A. Winick, J. J. Wallman, and J. Emerson, Phys. Rev. Lett. **126**, 230502 (2021).
[20] K. X. Wei, E. Magesan, I. Lauer, S. Srinivasan, D. F. Bogorin, S. Carnevale, G. A. Keefe, Y. Kim, D. Klaus, W. Landers, N. Sundaresan, C. Wang, E. J. Zhang, M. Steffen, O. E. Dial, D. C. McKay, and A. Kandala, Phys. Rev. Lett. **129**, 060501 (2022).
[21] H.-Y. Huang, R. Kueng, and J. Preskill, Nat. Phys. **16**, 1050 (2020).
[22] A. Elben, S. T. Flammia, H.-Y. Huang, R. Kueng, J. Preskill, B. Vermersch, and P. Zoller, Nat. Rev. Phys. **5**, 9 (2022).
[23] G. Chiribella, G. M. D'Ariano, and P. Perinotti, Phys. Rev. Lett. **101**, 180501 (2008).
[24] S. Shrapnel, F. Costa, and G. Milburn, New J. Phys. **20**, 053010 (2018).
[25] F. Costa, M. Ringbauer, M. E. Goggin, A. G. White, and A. Fedrizzi, Phys. Rev. A **98**, 012328 (2018).
[26] J. Helsen, M. Ioannou, I. Roth, J. Kitzinger, E. Onorati, A. H. Werner, and J. Eisert, arXiv:2110.13178.
[27] C. Hadfield, S. Bravyi, R. Raymond, and A. Mezzacapo, Commun. Math. Phys. **391**, 951 (2022).
[28] H.-Y. Huang, R. Kueng, G. Torlai, V. V. Albert, and J. Preskill, Science **377**, eabk3333 (2022).
[29] A. Elben, R. Kueng, H. Y. R. Huang, R. van Bijnen, C. Kokail, M. Dalmonte, P. Calabrese, B. Kraus, J. Preskill, P. Zoller, and B. Vermersch, Phys. Rev. Lett. **125**, 200501 (2020).
[30] See Supplemental Material at http://link.aps.org/supplemental/10.1103/PhysRevLett.130.160401 contains relevant background about process tensors, a proof that the protocol in the main text erases non-Markovian correlations due to other device qubits, and further details about the numerical experiments, which includes Ref. [31].
[31] C. J. Wood, J. D. Biamonte, and D. G. Cory, Quantum Inf. Comput. **15**, 0579 (2015) [arXiv:1111.6950].
[32] M. Sarovar, T. Proctor, K. Rudinger, K. Young, E. Nielsen, and R. Blume-Kohout, Quantum **4**, 321 (2020).
[33] K. Rudinger, C. W. Hogle, R. K. Naik, A. Hashim, D. Lobser, D. I. Santiago, M. D. Grace, E. Nielsen, T. Proctor, S. Seritan, S. M. Clark, R. Blume-Kohout, I. Siddiqi, and K. C. Young, PRX Quantum **2**, 040338 (2021).
[34] S. Milz and K. Modi, PRX Quantum **2**, 030201 (2021).
[35] H.-Y. Huang, M. Broughton, J. Cotler, S. Chen, J. Li, M. Mohseni, H. Neven, R. Babbush, R. Kueng, J. Preskill, and J. R. McClean, Science **376**, 1182 (2022).
[36] H.-Y. Huang, R. Kueng, and J. Preskill, Phys. Rev. Lett. **126**, 190505 (2021).
[37] I. A. Aloisio, G. A. L. White, C. D. Hill, and K. Modi, arXiv:2209.10870.
[38] I. A. Luchnikov, S. V. Vintskevich, D. A. Grigoriev, and S. N. Filippov, Phys. Rev. Lett. **124**, 140502 (2020).
[39] J. Cerrillo and J. Cao, Phys. Rev. Lett. **112**, 110401 (2014).
[40] P. Figueroa-Romero, K. Modi, R. J. Harris, T. M. Stace, and M.-H. Hsieh, PRX Quantum **2**, 040351 (2021).